Reactive Uptake of NO_3, N_2O_5, NO_2, HNO_3, and O_3 on Three Types of Polycyclic Aromatic Hydrocarbon Surfaces

Simone Gross and Allan K. Bertram*

Department of Chemistry, University of British Columbia, Vancouver, British Columbia, Canada V6T 1Z3

Received: November 9, 2007; In Final Form: January 9, 2008

We investigated the reactive uptake of NO_3, N_2O_5, NO_2, HNO_3, and O_3 on three types of solid polycyclic aromatic hydrocarbons (PAHs) using a coated wall flow tube reactor coupled to a chemical ionization mass spectrometer. The PAH surfaces studied were the 4-ring systems pyrene, benz[a]anthracene, and fluoranthene. Reaction of NO_3 radicals with all three PAHs was observed to be very fast with the reactive uptake coefficient, γ, ranging from 0.059 (+0.11/−0.049) for benz[a]anthracene at 273 K to 0.79 (+0.21/−0.67) for pyrene at room temperature. In contrast to the NO_3 reactions, reactions of the different PAHs with the other gas-phase species (N_2O_5, NO_2, HNO_3, and O_3) were at or below the detection limit ($\gamma \leq 6.6 \times 10^{-5}$) in all cases, illustrating that these reactions are at best slow. For NO_3 we also investigated the time dependence of the reactive uptake to determine if the surface-bound PAH molecules were active participants in the reaction (i.e., reactants). Reaction of NO_3 on all three PAH surfaces slowed down at 263 K after long NO_3 exposure times, suggesting that the PAH molecules were reactants. Additionally, NO_2 and HNO_3 were identified as major gas-phase products. Our results show that under certain atmospheric conditions, NO_3 radicals can be a more important sink for PAHs than NO_2, HNO_3, N_2O_5, or O_3 and impact tropospheric lifetimes of surface-bound PAHs.

Introduction

Polycyclic aromatic hydrocarbons (PAHs) are observed in environmental samples worldwide. Their occurrence in the atmosphere constitutes a health risk to the population due to their allergenic, mutagenic, and carcinogenic properties. Sources of PAHs are incomplete combustion processes such as diesel and gasoline engines and biomass or coal burning.[1] Concentrations of individual particle-phase PAHs in atmospheric samples are usually in the range of a few ng m^{-3} for urban areas around the world but can reach as high as 900 ng m^{-3} during heavy traffic conditions or biomass burning episodes.[1−8] Understanding the lifetime and fate of PAHs in the atmosphere is important for health risk assessments.

PAHs have a wide range of vapor pressures (e.g., the vapor pressure of the two-ring PAH naphthalene is 7.8×10^{-2} Torr, and that of coronene (seven aromatic rings) is 1.5×10^{-12} Torr).[1] As a result, PAHs are found both in the gas-phase (two- and three-ring PAHs) as well as on and in atmospheric particulate matter (PAHs with five and more aromatic rings). PAHs with three or four rings are semivolatile and observed both in the gas phase and adsorbed to particles. Additionally, aromatic compounds can also contribute to surface coatings on urban surfaces where aromatics account for ∼20% of the organic carbon mass of "urban grime" on buildings, windows, etc.[9,10] The fact that significant portions or the entirety of a PAH of higher molecular weight is found in the condensed phase shows the necessity to investigate not only gas-phase reactions of PAH molecules but also reactions between atmospheric oxidants and PAHs adsorbed on or in aerosol particles and urban surfaces. Reactions between gas-phase oxidants and surface-bound PAHs (which is often referred to as heterogeneous chemistry) may be
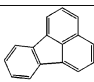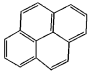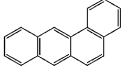
an important loss process of PAHs in the atmosphere and a source of even more toxic and mutagenic PAH derivatives.[1,11]

Up to now most scientific work on PAHs has focused on gas-phase homogeneous chemistry, with only a limited amount of work reported on heterogeneous reactions. However, the available data on heterogeneous chemistry suggests that, in general, heterogeneous reactions can differ dramatically from homogeneous reaction rates, mechanisms, and products.[1,12−15] Heterogeneous reactions between condensed phase PAHs and the following gas-phase oxidants have been explored: OH,[16−18] NO,[17] NO_2,[5,16,17,19−22] O_3,[15,23−28] HNO_3,[29] N_2O_5,[30,31] and NO_3.[30,32] In a number of these studies reactive uptake coefficients, a parameter often used to describe a heterogeneous process, were not determined. The reactive uptake coefficient (γ) is defined as the fraction of collisions with a surface that leads to reactive loss. Studies that focus on determining γ for the atmospheric oxidants mentioned above on a range of PAH surfaces would be beneficial. Heterogeneous reactions between NO_3 and PAHs and N_2O_5 and PAHs are two reactions that are especially in need of further study. For example, the reactive uptake coefficient of N_2O_5 on PAH surfaces has not been previously determined, and the reactive uptake coefficient of NO_3 has only been investigated in one study and with one type of PAH molecule at room temperature.[32]

To add to the relatively short list of studies on heterogeneous reactions between gas-phase oxidants and surface-bound PAHs, we investigated the reactive uptake coefficient of NO_3, N_2O_5, NO_2, HNO_3, and O_3 on three types of solid PAH surfaces using a coated wall flow tube reactor. The PAH surfaces that we studied were pyrene (PYR), benz[a]anthracene (BEN), and fluoranthene (FLU) surfaces, which are four-ring systems with vapor pressures between 9.2×10^{-6} and 2.1×10^{-7} Torr at 298 K (see Table 1). These PAHs are typically distributed between gas and particle phase more or less equally in the

Polycyclic Aromatic Hydrocarbon Surfaces

J. Phys. Chem. A, Vol. 112, No. 14, 2008 **3105**

TABLE 1: Polycyclic Aromatic Hydrocarbons Studied, Their Molecular Structures, Molecular Weights, Melting Points, Vapor Pressures, and Typical Tropospheric Concentrations

PAH	molecular structure	molecular weight [g mol^{-1}]	melting point [°C]	vapor pressure at 298 K [torr]	atmospheric concentration [ng m^{-3}]
Fluoranthene		202.3	111	9.2×10^{-6}	2.8 – 12.4
Pyrene		202.3	156	4.5×10^{-6}	0.54 – 38
Benz[a]anthracene		228.3	160	2.1×10^{-7}	0.25 – 5.59

atmosphere (depending on ambient conditions).[1] This work is a continuation of our previous study, where we investigated the reactive uptake coefficient of NO_3 on solid pyrene.[32] Understanding heterogeneous reactions on solid PAH surfaces is a first step toward understanding heterogeneous reactions of PAHs adsorbed on or in aerosol particles.

Experiments consisted of measuring the reactive uptake coefficient of the gas-phase oxidants on "fresh" (i.e., unreacted) PAH surfaces by monitoring the decay of the gas-phase reactants. Our studies are complimentary to many of the previous studies of PAH heterogeneous chemistry since in our experiments we monitor the loss of the gas-phase reactant whereas most of the previous studies monitored the loss of the PAH material. Since we studied the loss of a range of different atmospheric oxidants on the same PAH surfaces, a direct comparison between the oxidants was possible. From our measurements we show that for all the gas-phase oxidants studied, except for NO_3, the reactive uptake coefficient is small ($\leq 6.6 \times 10^{-5}$).

For the NO_3 heterogeneous reaction, we also investigated NO_3 uptake as a function of time to determine if this reaction was catalytic (i.e., a reaction takes place at the surface but the surface is not an active participant) or if the reaction rate decreased with time due to oxidation of the surface-bound PAH molecules. This information is needed for extrapolating laboratory results to the atmosphere. The time dependence of the NO_3 uptake on PAH surfaces has not been investigated in previous studies.

Additionally, for the NO_3 reaction, we carried out preliminary gas-phase product studies for the reaction of NO_3 with pyrene at room temperature to aid in the understanding of the reaction mechanism.

Below, the results from these studies are presented and the importance of the different gas-phase oxidants for removing PAHs by heterogeneous chemistry is discussed. One of the main conclusions is that NO_3 under certain conditions should be more important than all the other gas-phase oxidants studied for transforming PAHs heterogeneously. Another important conclusion is that the N_2O_5 heterogeneous reaction is not likely important for removing PAHs under many atmospheric conditions.

Experimental Section

Experimental Setup and Procedure. The apparatus used in this work was similar to that previously used in our laboratory to study heterogeneous loss processes.[32−34] It consisted of a coated-wall flow tube reactor coupled to a chemical ionization mass spectrometer (CIMS). The flow tube was constructed of borosilicate glass and included a movable injector through which the gas-phase reactant was introduced. The main carrier gas was introduced through a port at the upstream end of the flow reactor. The inside wall of a Pyrex tube (1.75 cm inside diameter and 11−15 cm in length) was coated with the PAH film and then inserted into the flow tube reactor. These coatings provided the surfaces for the heterogeneous studies. Total pressure in the flow reactor was 1.5−4.1 Torr. The flow was laminar in all experiments based on the Reynolds number. Reagent gases for chemical ionization were SF_6^- (for detecting N_2O_5, NO_3, NO_2, HNO_3, O_3, and HONO), I^- (for detecting NO_3), and O_2^+ (for detecting NO). Reagent ions were obtained by passing trace amounts of SF_6 in N_2, CH_3I in N_2, or O_2 in He through a ^{210}Po source to obtain SF_6^-, I^-, or O_2^+, respectively. Concentrations of the gas-phase oxidants used in our studies were $(0.8−5.7) \times 10^{12}$ molecule cm^{-3} for N_2O_5, $(0.3−3.7) \times 10^{11}$ molecule cm^{-3} for NO_3, $(2.0−9.6) \times 10^{13}$ molecule cm^{-3} for O_3, $(0.17−4.9) \times 10^{12}$ molecule cm^{-3} for HNO_3, and $(4.4−6.4) \times 10^{13}$ molecule cm^{-3} for NO_2. These concentrations were calculated using the corresponding rate constants of these species with SF_6^- or I^-. Uncertainties in these calculated concentrations, based on uncertainties in the rate constants, are 30−50%.[35]

Three different types of experiments were carried out. The first set of experiments involved measuring the reactive uptake coefficients of NO_3, NO_2, N_2O_5, O_3, and HNO_3 on "fresh" PAH surfaces at 273 K and room temperature. We refer to the reactive uptake coefficient on "fresh" (or unreacted) surfaces as the initial reactive uptake coefficient (γ_0), and we refer to these experiments as *measurements of the initial reactive uptake coefficients*. The initial reactive uptake coefficients γ_0 were determined from the irreversible removal of the gas-phase species as a function of injector position (and therefore reaction time). The slope of a plot of the natural logarithm of the gas CIMS signal versus the injector position was used to obtain the observed first-order loss rate, k_{obs}. This loss rate was corrected for concentration gradients close to the flow-tube wall[36] and then used to calculate γ_0 using a standard procedure.[33] This procedure assumes that the surface area available for reaction is equal to the geometric surface area of the Pyrex tubes. Below we show that this is a reasonable approximation. When measuring γ_0, the total exposure time of the surface to the gas-phase reactants was kept short and the concentrations of gas-phase reactants were kept small (see above for specific values) to minimize oxidation of the surface during measurements of γ_0.

The second set of experiments involved investigating the time dependence of the NO_3 reactive uptake to determine if this reaction was catalytic or if the reaction rate decreased with exposure time due to oxidation of the surface. We refer to these experiments as *processing studies*. For these measurements initially the tip of the injector was positioned at the front of the flow cell so the surface was not exposed to NO_3 radicals, and then a flow of NO_3 was established. Next, the injector was withdrawn quickly 5 cm so that the PAH surface was exposed to NO_3. The signal of NO_3 was then monitored for an extended period of time (60 min) to determine if the surface was deactivated or processed from prolonged exposure to NO_3. In contrast to experiments determining γ_0, these experiments were conducted in the presence of O_2 $((0.95−2.1) \times 10^{16}$ molecule cm$^{-3})$ to better mimic atmospheric conditions.

The third set of experiments involved measurements of gas-phase products for the reaction between NO_3 and pyrene at 297 ± 1 K. We refer to these experiments as *gas-phase product studies*. For these studies, release of NO_2, HNO_3, HONO, and NO to the gas phase during a 60 min NO_3 uptake experiment on pyrene was monitored with CIMS. The general procedure

was identical to the second set of experiments, but instead of monitoring the NO_3 signal, NO_2, HNO_3, HONO, and NO CIMS signal intensities were monitored during 60 min of NO_3 exposure.

Chemicals. Pyrene (purity 95%), benz[a]anthracene (99%), and fluoranthene (99%) were purchased from Sigma-Aldrich and used without further purification. NO_2 (99.5%) was purchased from Matheson; N_2 (99.999%), O_2 (99.993%), and He (99.999%) were purchased from Praxair. Gas-phase nitric acid was produced by flowing He over an aqueous solution containing nitric acid and sulfuric acid at ~197 K. This solution was prepared by combining an aqueous solution of nitric acid (69 wt %, Fisher Scientific) and sulfuric acid (96 wt %, Fisher Scientific) in a 3:1 ratio by volume.[37] Ozone was generated by passing O_2 through an ultraviolet light source. N_2O_5 was generated by reacting NO_2 with an excess amount of O_3 in a flow system as described by Schott et al.[38] and Knopf et al. (Knopf, Cosman et al., *J. Phys. Chem. B* **2007**, *111*, 11021−11032.) The solid N_2O_5 crystals were stored at 197 K. NO_3 radicals were obtained by thermal conversion of gaseous N_2O_5 to NO_3 and NO_2 at 430 K in a Teflon-coated glass oven.[32,34]

Preparation and Characterization of PAH Films. Solid PAH films were prepared by first distributing solid PAH powder on the inner wall of glass cylinders with an inner diameter of 1.75 cm (for experiments in the flow reactor) or on planar glass slides (for film characterization using scanning electron microscopy (SEM) and profilometry). The glass cylinders or slides were then heated to a temperature just above the melting point of the corresponding PAH material (see Table 1). Rotation of the cylinder ensured even distribution of the molten PAH. The PAHs rapidly crystallized upon cooling, resulting in a relatively smooth film, as discussed below. To test whether the reactive uptake coefficient depended on the method of film preparation, we also prepared some pyrene films by dissolving pyrene in xylene; then this solution was applied to the inside walls of the glass cylinder, and the solvent was allowed to evaporate, leaving behind a coating of pyrene.

To characterize the PAH surfaces, we recorded images of PAH films using SEM, and we measured the roughness using profilometry. The SEM and profilometry measurements were performed using glass slides rather than Pyrex tubes. However, the slides were prepared using the same techniques that were used to prepare the glass cylinders. SEM pictures were obtained using a Hitachi S-3000N scanning electron microscope, and profilometer scans were taken with a Tencor alpha-step 200 profilometer.

Results and Discussion

Surface Properties of PAH Films. As mentioned above, to assess the surface properties of the PAH films, SEM and profilometer measurements were conducted. The electron microscope images (see Figure 1) confirmed that the PAH films were relatively smooth, nonporous, and completely covered the glass substrate. The profilometer measurements indicated that the surface area of these films deviated from the surface area of the glass substrate by a maximum of 2%, indicating the films were smooth. Therefore, when calculating γ_0 we assumed the surface area available for heterogeneous reactions was equal to the geometric surface area of the Pyrex tubes as discussed above.

Measurements of the Initial Reactive Uptake Coefficients for NO_3. As mentioned above, the reactive uptake coefficients on "fresh" surfaces were determined from the irreversible removal of the gas-phase species as a function of injector position. Shown in Figure 2 is an example of the raw data from
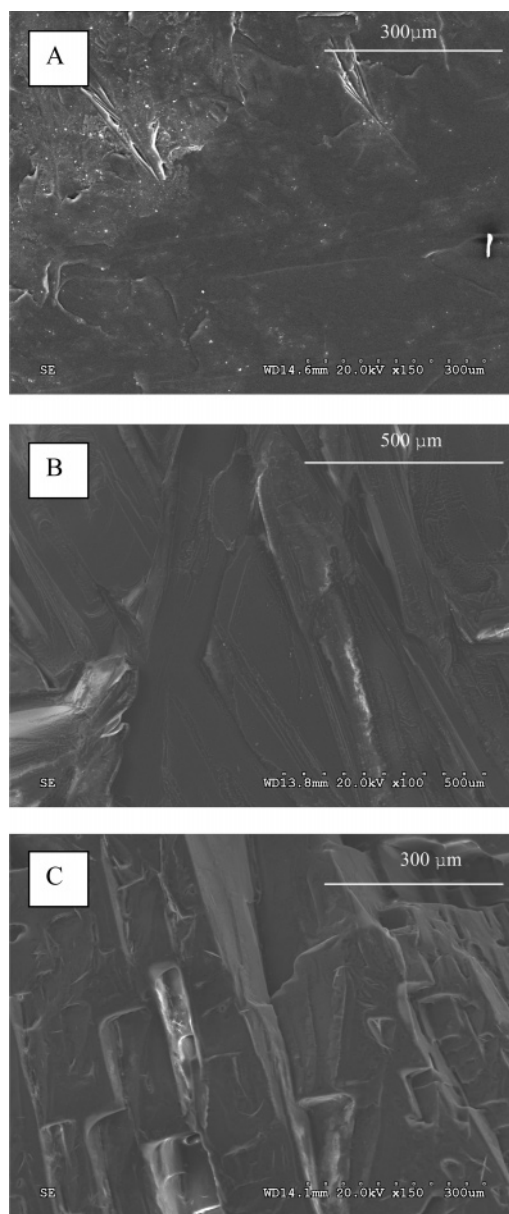

Figure 1. Scanning electron microscope images of solid PAH surfaces (A, benz[a]anthracene; B, fluoranthene; C, pyrene).

a typical measurement with NO_3. This plot shows that NO_3 interacted strongly with the PAH surface and also that loss of the NO_3 signal was irreversible.

A typical plot for the natural logarithm of the normalized NO_3 signal versus injector position for PYR is shown in Figure 3. The slope of this plot was then used to calculate γ_0. Listed in Tables 2 and 3 are the γ_0 values for NO_3 on PYR, FLU, and BEN obtained at 273 K and room temperature. The reported uncertainties include uncertainties in the diffusion coefficient of NO_3 in helium of 7.2%.[39] Our previous paper showed that the reactive uptake coefficient of NO_3 on pyrene at 293 K is large. The data in Tables 2 and 3 show that the reactive uptake coefficient of NO_3 on two other PAHs is also large and that the temperature dependence of the uptake coefficient over the range of 273−298 K is small.

Note, the PAHs investigated in our study have a very low vapor pressure and the homogeneous reaction of PAHs with NO_3 in the gas phase is slow. Hence, the gas-phase reaction between NO_3 and PAHs did not influence our heterogeneous studies. Specifically, the gas-phase reaction will contribute less
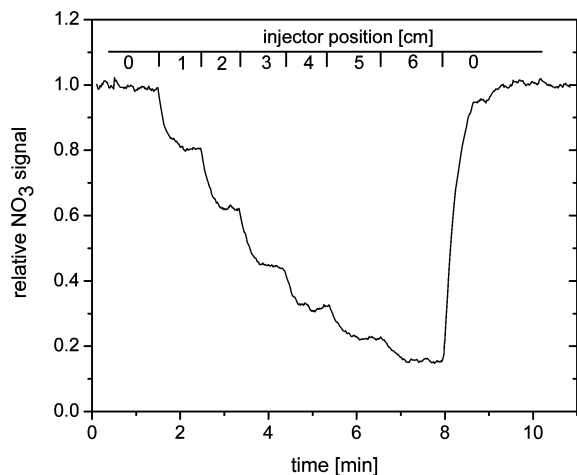
Polycyclic Aromatic Hydrocarbon Surfaces

J. Phys. Chem. A, Vol. 112, No. 14, 2008 **3107**

Figure 2. NO$_3$ signal as a function of time for a typical uptake experiment of NO$_3$ on fluoranthene at 273 K. Each step down corresponds to an increase of the reactive surface (i.e., the injector is pulled back in 1 cm increments). At the end, the signal recovers as the injector is pushed back to its original position ("0" position, no exposure). Scale within the graph corresponds to the positions of the NO$_3$ injector during the different steps of the experiment.
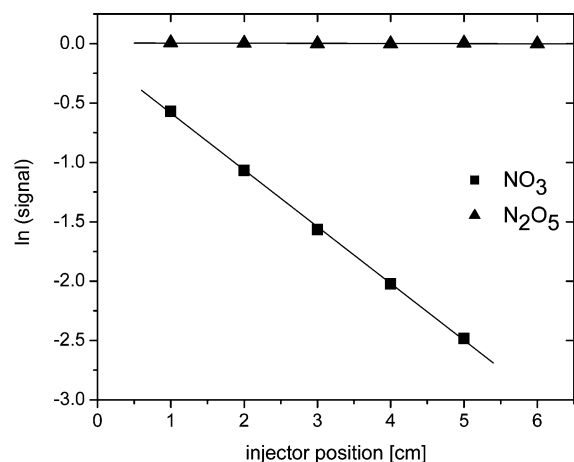

Figure 3. Plot of the natural logarithm of the CIMS signals vs the injector position for NO$_3$ and N$_2$O$_5$ during typical experiments on pyrene solid surfaces at 273 K.

than 1% to the total loss of NO$_3$ in our experiments, based on saturated vapor pressures of the PAH material and the rate coefficients for the gas-phase NO$_3$−PAH homogeneous reactions.[1]

We also carried out some tests to determine if the method of preparing the films or the presence of O$_2$ in the flow reactor influenced the reactive uptake coefficients. Within the uncertainty of our measurements, the reactive uptake coefficient of NO$_3$ on pyrene did not depend on the presence of O$_2$ in the flow reactor at room temperature. Also, within the uncertainty of our measurements, the reactive uptake coefficient measured at 273 K for NO$_3$ was the same on pyrene surfaces prepared by melting pyrene crystals and on pyrene surfaces prepared by dissolving pyrene crystals in xylene and then coating the Pyrex tubes with the resulting solution. In short, the reactive uptake coefficients appeared to be independent of the method of preparing the films and also the presence of O$_2$ in the flow reactor.

To compare the rate of the reaction between NO$_3$ and pyrene on a surface with the same reaction in the gas phase, we calculated an enhancement factor for the surface reaction, similar

to Moise and Rudich.[12] The enhancement factor is defined as follows

$$R = \frac{\text{surface reaction probability}}{\text{gas-phase reaction probability}} = \frac{\gamma}{k_{\text{gas−phase}}/10^{-10}} \quad (1)$$

The gas-phase reaction rate for NO$_3$, $k_{\text{gas−phase}}$, depends on NO$_2$ concentrations.[1,40] Using a NO$_2$ concentration of 10 ppb, $k_{\text{gas−phase}}$ for NO$_3$ with PYR and FLU is 4×10^{-16} and 1×10^{-16} cm^3 molecule^{-1} s^{-1} at room temperature, respectively.[1,40] Using these values and our measured reactive uptake coefficients from Table 3 in eq 1, we obtain R values for room temperature of 2×10^5 and 9×10^4 for PYR and FLU, respectively. This suggests that the surface reaction is enhanced by approximately 5 orders of magnitude. Enhancement of reactions on surfaces compared to their analogous gas-phase reactions has also been observed previously. For O$_3$ with aliphatic unsaturated surfaces enhancement factors ranging from 10 to 1000 were observed.[12,13] Also, for O(^{3}P) with aliphatic saturated surfaces, Br with aliphatic saturated surfaces, and NO$_3$ on aliphatic surfaces enhancement factors of 10^3, 10^4, and 100 were observed, respectively.[12] Possible explanations of these results are longer residence times of the gas-phase species at a surface compared to a homogeneous encounter in the gas phase, a lowering of the activation energy barrier of the reaction, or a new reaction channel on the surface that is inaccessible in the gas phase.[12,13,41,42] Research is needed to better understand these drastic enhancement factors.

As mentioned in the Introduction, in many previous heterogeneous studies with PAHs the reactive uptake coefficient was not determined. Rather, the time to react away a fraction of the surface-bound PAH molecules was determined. To compare our results with these previous measurements, we converted both our measurements and the previous measurements (when γ was not determined) into an atmospheric lifetime with respect to heterogeneous chemistry, τ_{atm}. This lifetime is defined as the time in which 63% of the molecules react and can be thought of as the processing time of a surface-bound PAH molecule. To convert our measurements into an atmospheric lifetime we used the following equation[12]

$$\tau_{\text{atm}} = \frac{4N_{\text{tot}}}{\gamma_0 c_{\text{avg}}[\text{oxidant}]_{\text{atm}}} \quad (2)$$

where N_{tot} is the surface concentration of PAH molecules (molecule cm^{-2}), c_{avg} is the mean thermal velocity (cm s^{-1}), and [oxidant]$_{\text{atm}}$ is the typical concentration of the gas-phase oxidants in the atmosphere. To translate our measured γ_0 into τ_{atm} we used a surface density of 1×10^{14} reactive sites cm^{-2}, which is consistent with numbers in the literature.[24] The values for [oxidant]$_{\text{atm}}$ used in these calculations are listed in Tables 2 and 3. To convert the previous laboratory studies, where the decay of surface-bound PAH molecules was monitored into τ_{atm}, we used the following equation

$$\tau_{\text{atm}} = \tau_{\text{lab}}\frac{[\text{oxidant}]_{\text{lab}}}{[\text{oxidant}]_{\text{atm}}} \quad (3)$$

where τ_{lab} is the average lifetime of surface-bound PAH species determined in the laboratory. In cases where τ_{lab} was not mentioned we estimated this value based on the reported experimental data. [oxidant]$_{\text{lab}}$ is the concentration of the gas-phase oxidant used in the laboratory experiments. This equation assumes the lifetime of surface-bound PAH species is linear

TABLE 2: Results of the Uptake Experiments at 273 K[a]

	[oxidant]$_\text{atm}$[b]	reactive uptake coefficient γ_0			γ_0 [oxidant]$_\text{atm}$/molecule cm^{-3}	τ_atm[c]
		BEN	FLU	PYR	PYR	PYR
NO$_3$	50 ppt	$0.059\,^{+0.11}_{-0.049}$	$0.52\,^{+0.48}_{-0.45}$	$0.38\,^{+0.62}_{-0.30}$	$\geq 4.8 \times 10^8$	≤ 28 s
N$_2$O$_5$	10 000 ppt	$\leq 2.1 \times 10^{-6}$	$\leq 8.7 \times 10^{-6}$	$\leq 4.9 \times 10^{-6}$	$\leq 1.2 \times 10^6$	≥ 4 h
NO$_2$	100 000 ppt	$\leq 1.0 \times 10^{-6}$	$\leq 4.5 \times 10^{-7}$	$\leq 5.7 \times 10^{-7}$	$\leq 1.4 \times 10^6$	≥ 2.2 h
HNO$_3$	10 000 ppt	$\leq 2.4 \times 10^{-5}$	$(8.6 \pm 2.3) \times 10^{-6}$	$\leq 2.7 \times 10^{-5}$	$\leq 6.8 \times 10^6$	≥ 32 min
O$_3$	100 000 ppt	$\leq 1.6 \times 10^{-6}$	$\leq 5.7 \times 10^{-7}$	$\leq 9.7 \times 10^{-7}$	$\leq 2.4 \times 10^6$	≥ 1.3 h

[a] Uptake coefficients of N$_2$O$_5$, NO$_2$, HNO$_3$, and O$_3$ are reported as upper limits. Uptake coefficients of NO$_3$ on PAHs reported with upper limit of 1 indicate that these experiments were diffusion limited. [b] Typical atmospheric concentration; converted into total molecules cm^{-3} for calculations in last two columns.[1] [c] Atmospheric lifetime of pyrene at an oxidant concentration equal to the concentration given in column [oxidant].

TABLE 3: Results of the Uptake Experiments at 293−297 K[a]

	[oxidant]$_\text{atm}$[b]	reactive uptake coefficient γ_0			γ_0 [oxidant]$_\text{atm}$/molecule cm^{-3}	τ_atm[c]
		BEN	FLU	PYR	PYR	PYR
NO$_3$	50 ppt	$0.13\,^{+0.53}_{-0.096}$	$0.087\,^{+0.28}_{-0.063}$	$0.79\,^{+0.21}_{-0.67}$	$\geq 9.9 \times 10^8$	≤ 13 s
N$_2$O$_5$	10 000 ppt	$\leq 5.7 \times 10^{-6}$	$\leq 8.5 \times 10^{-6}$	$\leq 4.1 \times 10^{-6}$	$\leq 1.0 \times 10^6$	≥ 4.6 h
NO$_2$	100 000 ppt	n.d.	n.d.	$\leq 1.0 \times 10^{-6}$	$\leq 2.5 \times 10^6$	≥ 1.2 h
HNO$_3$	10 000 ppt	n.d.	n.d.	$\leq 6.6 \times 10^{-5}$	$\leq 1.7 \times 10^7$	≥ 13 min
O$_3$	100 000 ppt	n.d.	n.d.	$\leq 7.6 \times 10^{-7}$	$\leq 1.9 \times 10^6$	≥ 1.6 h

[a] See Table 2 for explanations. n.d.= not determined. [b] Typical atmospheric concentration; converted into total molecules cm^{-3} for calculations in last two columns.[1] [c] Atmospheric lifetime of pyrene at an oxidant concentration equal to the concentration given in column [oxidant].

with the concentration of the gas-phase oxidant over the extrapolation range.

More than 20 years ago in a pioneering study, Pitts et al.[30] investigated the reaction of NO$_3$ with pyrene and perylene adsorbed on glass fiber filters in an environmental chamber. In these experiments, the amount of PAH material used resulted in less than a monolayer coverage on the filters. The authors monitored the decay of the PAH material rather than the loss of NO$_3$, and an NO$_3$ concentration of approximately 2.5×10^{11} molecule cm^{-3} was used. Under these conditions, the authors concluded that neither adsorbed pyrene nor perylene reacted to any observable extent with the NO$_3$ radical over a time period of 50 min. On the basis of these values and eq 3, we calculate an atmospheric lifetime τ_atm of >167 h at 50 ppt NO$_3$. In contrast, from our experimental results and eq 2 we estimate an atmospheric lifetime of 13 s. A possible reason for the apparent discrepancy between our results and the results presented by Pitts et al. may be the difference in experimental conditions. As we discussed in our previous publication,[32] the experiments by Pitts et al. were carried out in the presence of large concentrations of N$_2$O$_5$ (3.8×10^{13} molecule cm^{-3}). These large concentrations may have interfered with the surface reaction between NO$_3$ and pyrene by blocking reaction sites. Additionally, it is known that different underlying substrates for PAHs result in different reaction rates for O$_3$[14,23,24,26,27] and NO$_2$[21]. This might also be true for NO$_3$. Pitts et al.[30] used PAHs on filter substrates, while solid PAH surfaces were used in this study.

The recent aerosol studies by Schauer et al.[43] may also be related to our NO$_3$ studies. These authors studied the decay of benzo[a]pyrene (BaP) on spark discharge soot particles exposed to ozone. Upon addition of NO$_2$ they saw an enhanced loss of BaP, whereas the NO$_2$ alone did not result in loss of BaP. As indicated by the authors, the enhanced loss was attributed to formation of reactive intermediates such as NO$_3$. In other words, the measurements by Schauer et al. are consistent with a significant reaction between NO$_3$ and surface-bound BaP, although reaction rates were not quantified.

Measurements of the Initial Reactive Uptake Coefficients for N$_2$O$_5$. The reactive uptake coefficients for N$_2$O$_5$ on fresh PAH surfaces were determined in the same way as NO$_3$ uptake coefficients. Shown in Figure 3 is an example of data obtained for N$_2$O$_5$ loss on pyrene. For this case the change in the N$_2$O$_5$ signal was less than the scatter in the data. In fact, for all PAH surfaces investigated and for both temperatures (273 K and room temperature), the change in the N$_2$O$_5$ signal was less than the uncertainty in the measurements. From the data we estimated an upper limit of γ_0, and these values are listed in Tables 2 and 3. These upper limits are based on the 95% confidence interval of our experimental results. As shown, the reactive uptake coefficients are small and drastically less than the reactive uptake coefficients of NO$_3$ on the same surfaces.

Two previous studies investigated the reactions of N$_2$O$_5$ on PAH surfaces; however, reactive uptake coefficients were not measured.[30,31] Our study is the first to report the reactive uptake coefficients of N$_2$O$_5$ on PAH surfaces. We can nevertheless compare our results with theirs using atmospheric lifetimes as discussed above. Our results and eq 2 lead to an atmospheric lifetime of ≥ 4.6 h at room temperature, and the results from Pitts et al. and Kamens et al. and eq 3 lead to atmospheric lifetimes of 100 h (Pitts et al.)[30] and 222 h (Kamens et al.).[31] These calculations show that our results do not contradict the previous measurements.

Measurements of the Initial Reactive Uptake Coefficients for O$_3$. Uptake coefficients γ_0 were obtained for O$_3$ in the same way as for NO$_3$ and N$_2$O$_5$. Similar to N$_2$O$_5$, the decrease in the CIMS signal was less than the scatter in the O$_3$ data. From the measurements we calculated an upper limit of γ_0 based on the 95% confidence interval of our experimental results (see Tables 2−4).

In Table 4 we compare our results with results obtained in previous studies. In cases where reactive uptake coefficients were not measured, we determined τ_atm from the experimental data and eq 3 and included these values for comparison. Note that our results were obtained by monitoring the loss of the gas-phase reactant, while the previous measurements were obtained by monitoring the decay of PAH molecules. Differences may be due to different substrates (see above) and different PAHs used. However, as can be seen in columns for

Polycyclic Aromatic Hydrocarbon Surfaces

J. Phys. Chem. A, Vol. 112, No. 14, 2008 **3109**

TABLE 4: Summary of Measurements of O$_3$ Uptake on PAH Surfaces[a]

ref	surface	temp.	γ_0	τ_{atm}
this study	solid PYR	273 K	$\leq 9.7 \times 10^{-7}$	≥ 1.3 h
	solid FLU		$\leq 5.7 \times 10^{-7}$	
	solid BEN		$\leq 1.6 \times 10^{-6}$	
this study	solid PYR	293–297 K	$\leq 7.6 \times 10^{-7}$	≥ 1.6 h
Poschl et al.[23]	BaP on soot[b]	298 K	$\sim 2 \times 10^{-5}$ to 2×10^{-6}	
Kwamena et al.[24]	BaP on solid organic aerosol[b]	298 K	$\sim 2 \times 10^{-6}$ to 5×10^{-7}	
Mmereki et al.[15,25]	anthracene at air–water interface[c]	298 K	$\sim 3 \times 10^{-7}$ to 2×10^{-8}	
Van Vaeck and Van Cauwenberghe[28]	BEN	room temperature		11 h
Pitts et al.[27]	PYR	room temperature		~ 4–5 h
	FLU			~ 6–9 h
	BEN			~ 4–> 9 h
	BaP on filters			~ 4–9 h
Alebic-Juretic et al.[26]	PYR	room temperature		~ 1.4 h
	FLU			~ 17 h
	BEN			~ 0.7 h
	on silica gel			

[a] For calculations of lifetimes (τ_{atm}), O$_3$ concentrations of 100 ppb were used for all studies for comparison purposes. [b] The reactive uptake coefficient depended on relative humidity and O$_3$ concentrations. [c] The reactive uptake coefficient depended on O$_3$ concentration and whether or not the air–water interface was coated with an organic monolayer.

γ_0 and the atmospheric lifetime calculated with 100 ppb O$_3$, our data are broadly consistent with the previous measurements.

Measurements of the Initial Reactive Uptake Coefficients for NO$_2$. Our measured reactive uptake coefficients γ_0 for NO$_2$ were $\leq 1.0 \times 10^{-6}$ for all three PAHs at 273 K and at room temperature (see Tables 2 and 3) (based on the 95% confidence interval of our experimental results). The only other study that has investigated the reactive uptake coefficient of NO$_2$ on PAH surfaces was the work by Arens et al.[19] These authors studied the uptake on a solid layer of anthrarobin adsorbed onto a glass substrate. They obtained γ values of 7×10^{-7}–2×10^{-6} at different NO$_2$ concentrations and relative humidities, which is in general consistent with our numbers. Esteve et al.[16,17] also studied NO$_2$ heterogeneous reactions on 13 different PAHs adsorbed on graphite or diesel particles. Their experimental results and eq 3 leads to calculated atmospheric lifetimes τ_{atm} of PAHs ranging from 1.1 to 5.6 h, which is in the same range as the lifetimes calculated for PYR in this study (≥ 1.2 h).

Measurements of the Initial Reactive Uptake Coefficients for HNO$_3$. The upper limit reported for HNO$_3$ is slightly higher than those of N$_2$O$_5$, NO$_2$, and O$_3$ (see Tables 2 and 3). This is due to the fact that in some cases we observed a small uptake of HNO$_3$, which was at least partially reversible. Shown in Figure 4 is an example of the CIMS raw data obtained in a typical HNO$_3$ experiment. Shown is the HNO$_3$ signal as the injector is pulled back in equal 1 cm increments and then pushed forward to its original position. When the injector was returned to the starting position, the HNO$_3$ signal was larger than originally at the beginning of the experiment, indicating desorption of HNO$_3$ from the PAH surface. This indicates that at least part of the loss of HNO$_3$ was due to physical adsorption on the PAH surface. Since at least part of the loss of the HNO$_3$ signal was due to physical adsorption rather than reaction, the reactive uptake coefficients for HNO$_3$ determined in our experiments (based on the 95% confidence interval of our experimental results) should be considered as upper limits. Physisorption probably occurred to some extent for all the oxidants used in this study, but only HNO$_3$ showed physisorption at a detectable amount in our experiments, most likely due to the polarity of the molecule. Strong physisorption of HNO$_3$ has also been observed on soot.[37,44]

To the best of our knowledge, no other group has measured the reactive uptake coefficient of HNO$_3$ on PAH surfaces. However, experiments studying the reactivity of HNO$_3$ with PAHs have been performed by various researchers. Nielsen[45]
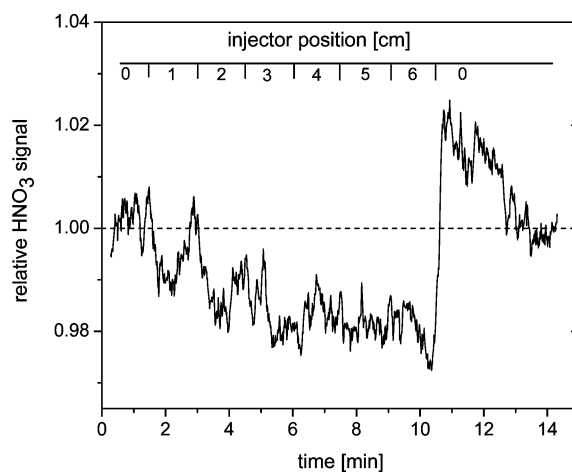

Figure 4. HNO$_3$ signal as a function of time for a typical uptake experiment of HNO$_3$ on fluoranthene at 273 K. Within the first 10 min the injector is pulled back in 1 cm increments, 6 cm total. At the end (at approximately 10 min), the signal increases compared to its original intensity as the injector is pushed back to its original position ("0", no exposure) and finally decreases to the original intensity. Scale within the graph corresponds to the positions of the injector during the different steps of the experiment.

studied the reactions of 25 PAHs with HNO$_3$ in mixed aqueous and organic solutions and observed PAH half-lives ranging from minutes to years. Vione et al.[46] studied heterogeneous reactions between HNO$_3$ and naphthalene in aqueous solution. They concluded that nitration with HNO$_3$ in the liquid phase is unlikely to occur in most environments. Similarly, in experiments by Pitts et al.[30] HNO$_3$ did not react significantly with PYR or perylene. These results are in agreement with our current measurements. The half-life reported in Kamens et al.[31] for BaP on wood soot with HNO$_3$ converts to an atmospheric lifetime of 161 days at typical tropospheric HNO$_3$ concentrations of 10 ppb. Our lower limits for the atmospheric lifetime do not contradict the previous measurements (see Tables 2 and 3).

Processing Studies of NO$_3$ (i.e., Uptake of NO$_3$ as a Function of Exposure). For these measurements, initially the tip of the injector is pushed to the front of the flow cell so the surface is not exposed to NO$_3$. Next, the injector is withdrawn quickly 5 cm, exposing 27.5 cm^2 of PAH film to NO$_3$. The NO$_3$ signal was then monitored for 60 min to determine if the surface is deactivated or processed from exposure to the gas-phase reactant. NO$_3$ concentrations used in these experiments
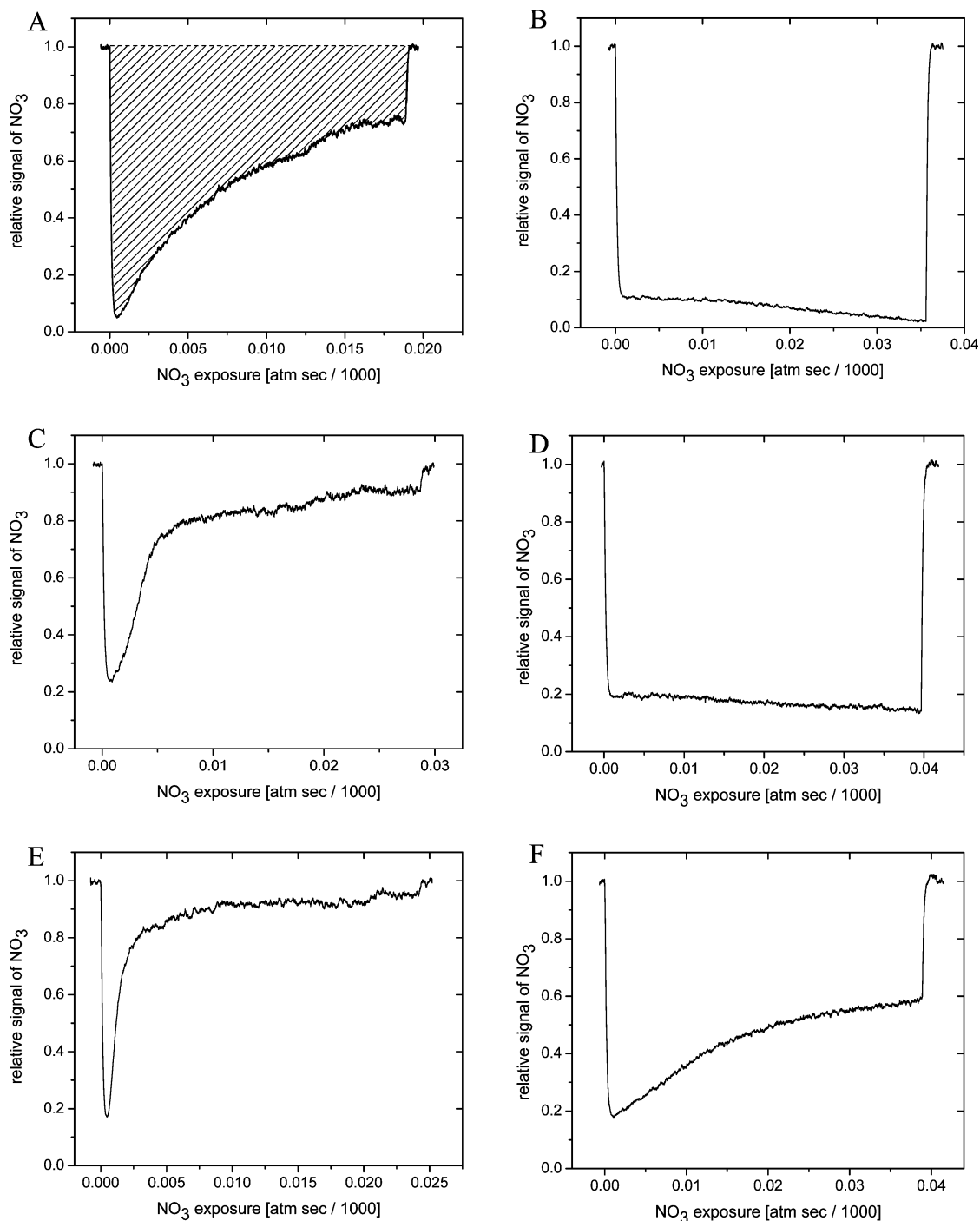
Figure 5. Relative changes of the NO_3 signal during exposure of PAH surfaces (27.5 cm²) to NO_3 for 60 min. NO_3 exposure corresponds to the product of NO_3 concentration and exposure time: (A and B) pyrene, (C and D) fluoranthene, and (E and F) benz[a]anthracene. Left-hand side (A, C, E): 263 ± 2 K. Right-hand side (B, D, F): 297 ± 3 K. The shaded region in A corresponds to the area integrated to determine the number of NO_3 radicals lost during the whole exposure experiment.

were $(1.3-3.4) \times 10^{11}$ molecule cm⁻³. All exposure studies were carried out in the presence of $(0.95-2.1) \times 10^{16}$ molecule cm⁻³ of O_2. Experiments were carried out at both 297 ± 3 and 263 ± 2 K. The lower temperature was chosen to minimize volatilization of PAHs and the products of the NO_3 and PAH reaction. A temperature of 263 K was used rather than 273 K in order to reduce the volatilization as much as possible. This prohibited replenishment of "fresh" PAH surfaces and enabled studying the "aging" of the PAH films.

Results from the processing studies are shown in Figure 5. In this figure NO_3 was normalized to the initial signal intensity before exposure to PAH and the product of the NO_3 concentra-

tion and exposure time (i.e., $[NO_3]t$) was plotted on the *x* axis rather than just exposure time, since processing is expected to be proportional to both concentration and exposure time.

Shown in Figure 5 are results carried out at 263 ± 2 K (panels A, C, and E) and 297 ± 3 K (panels B, D, and F). At 263 K, the NO_3 signal decreased drastically when the injector was pulled back, indicating a fast initial uptake. However, the signal slowly approached the initial value (relative signal = 1) over the period of 60 min, indicating that the reaction slowed down and the surface was being processed or deactivated. This suggests that the surface-bound PAH molecules were active participants in the reaction (i.e., reactants). Observations of the

change in color of the PAH surface with long exposures to NO_3 are also consistent with the conclusion that surface-bound PAH molecules were being oxidized. The surfaces changed from yellow/beige to red/brown during NO_3 exposure.

From the plots shown in Figure 5 we can determine the total number of NO_3 radicals lost to the surface at 263 K during the 60 min exposure by integrating the loss of the NO_3 signal over the entire exposure time using plots A, C, and E. The plot area of the depleted signal relative to the initial signal intensity (an example is shown for plot A as a gray shaded area) as well as experimental gas flows, concentrations in the flow cell, and the geometric surface area of the PAH films allowed us to calculate the total NO_3 uptake per unit area of PAH. The total number of NO_3 radicals lost to the PAH surfaces during the 60 min exposures were 4×10^{16}, 2×10^{16}, and 9×10^{15} NO_3 radicals cm^{-2} on PYR, FLU, and BEN, respectively. The fact that the number of NO_3 radicals lost per cm^2 is greater than the total number of surface PAH molecules per cm^2 is possibly because some of the condensed phase products of the heterogeneous reactions evaporated during the 60 min experiments, exposing a new (i.e., unreacted) PAH surface. Alternatively, some of the NO_3 radicals may diffuse into the bulk and react with subsurface PAH molecules. In other words, the bulk reaction may also contribute to our overall net loss of gas-phase radicals at extended exposure times. It is also possible that more than one NO_3 radical reacted with one surface PAH molecule.

Also from the plots in Figure 5 we can estimate the reactive uptake coefficient at the end of the exposure studies. First, the k_{obs} at the end of the exposure studies was calculated using the relative NO_3 signal just before the end of the 60 min exposure and a reaction length of 5 cm (i.e., the signal change during the movement of the injector from 5 cm exposure back to its "0" position). Then the reactive uptake coefficient was calculated from k_{obs}, as described in the Experimental Section. At the end of the 60 min exposure periods at 263 K, γ_{NO3} on PYR, FLU, and BEN decreased to 5×10^{-3}, 1×10^{-3}, and 6×10^{-4}, respectively.

In the processing studies, the trend observed at 297 K was drastically different than the trend observed at 263 K. The NO_3 signal did not recover for the experiments with PYR and FLU even up to NO_3 exposures of 0.04 atm s/1000 (equivalent to approximately 65 ppt NO_3 for 1 week). For the full 60 min experiment the NO_3 signal remained constant within experimental uncertainty. For the BEN surface at room temperature, there was partial recovery of the NO_3 signal but much less than at 263 K.

At 297 K during the 60 min exposure, the amount of NO_3 radicals lost per cm^2 to the surface was 5×10^{16}, 5×10^{16}, and 3×10^{16} for PYR, FLU, and BEN, respectively. Again, this is greater than a monolayer of PAHs on the surface, indicating that multilayers of the PAHs were reacted. One possible explanation for the continuous loss of NO_3, even after a monolayer of the PAHs (the surface layer) is reacted, is likely because the condensed phase products of the heterogeneous reactions evaporated during the exposure studies. The difference between 263 and 297 K is likely due to the higher volatility of condensed phase products at room temperature compared to 263 K.

Experiments were also performed at 273 K using PYR, and an intermediate behavior between the data at 263 and 297 K was observed (data not shown).

At room temperature, we observed that the NO_3 signal partially recovered for BEN surfaces during the processing studies, but the signal did not recover for PYR and FLU (see
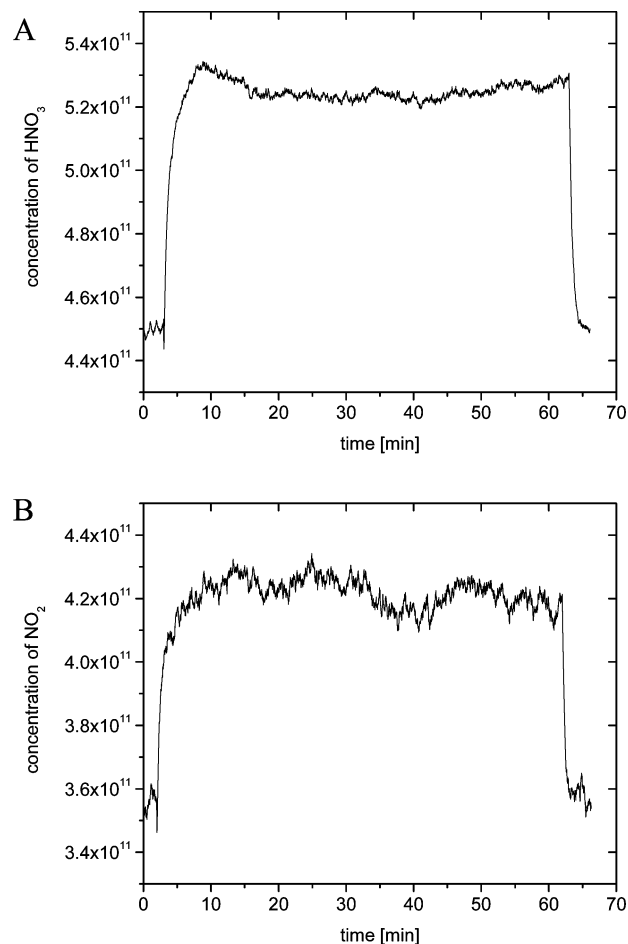

Figure 6. Changes in concentrations of HNO_3 (A) and NO_2 (B) during exposure of pyrene surfaces (27.5 cm^2) to NO_3 for 60 min at 297 $\pm$ 1 K. NO_3 concentrations exposed to the surfaces were approximately 2.5 $\times 10^{11}$ molecules cm^{-3}.

Figure 5B, D, F). This trend can also be explained using a similar argument to the one presented above. BEN has the lowest vapor pressure of the three PAHs investigated, and as a result one would expect the condensed phase products of this reaction to have a lower vapor pressure than the condensed phase products for the other two PAHs. If the products of the BEN reaction have a lower vapor pressure and remain on the surface, one would expect the NO_3 signal to recover faster in these experiments, which is the trend observed.

Gas-Phase Product Studies for Reaction of NO_3 with Pyrene. As mentioned above, we also carried out preliminary gas-phase product studies for the NO_3−pyrene reaction at 297 $\pm$ 1 K. In these studies we focused on HNO_3, NO_2, HONO, and NO, since our CIMS and chemical ionization schemes were sensitive to these species. In short, potential gas-phase products (HNO_3, NO_2, HONO, and NO) were monitored using CIMS, while a pyrene surface was exposed to NO_3. In Figure 6 we present some of the results from these experiments. For these measurements, initially the tip of the injector was pushed to the front of the flow cell so the surface was not exposed to NO_3. Next, the injector was withdrawn quickly 5 cm (at time = approximately 2.5 min), exposing 27.5 cm^2 of PAH film to NO_3. Plotted are the HNO_3 and NO_2 signals observed when the pyrene surface was exposed to an NO_3 concentration of approximately 2.5 $\times 10^{11}$ molecule cm^{-3}. Signal intensities of NO_2 and HNO_3 increased when NO_3 radicals were exposed to pyrene, while signal intensities of HONO and NO (data not shown) remained constant within experimental uncertainties.
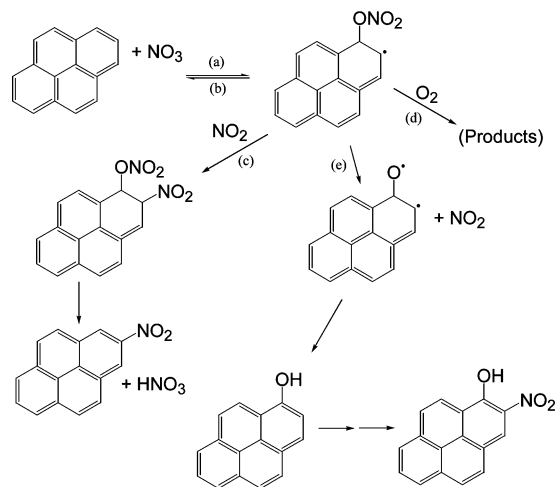
Figure 7. Suggested mechanism for the surface reaction of pyrene with NO₃ based on gas-phase chemistry of PAHs with NO₃. Note that other isomers may be formed as well.

During the 60 min experiments, $(1.6 \pm 0.5) \times 10^{16}$ NO₂ radicals and also $(1.6 \pm 0.5) \times 10^{16}$ HNO₃ molecules were produced per cm² of pyrene surface in the flow cell in the presence of O₂, while $(5 \pm 2) \times 10^{16}$ NO₃ radicals per cm² of surface were lost. Considering the mass balance of nitrogen, approximately one-third of the total nitrogen exposed to the surface (in the form of NO₃) reacted and stayed on the surface, most likely forming condensed phase products like nitro-pyrenes. More on the possible reaction mechanism is included below.

Proposed Reaction Mechanism for Reaction of NO₃ on Pyrene. The mechanisms for NO₃−PAH surface reactions are unknown. As a starting point, we assume that the NO₃−PAH reactions that occur in the gas phase can also occur on the surface, although the relative importance of the pathways may be significantly different. Shown in Figure 7 is a suggested mechanism based on gas-phase chemistry of PAHs with NO₃.[47−50] The possible pathways are as follows: first, addition of NO₃ radicals to the carbon atoms of the aromatic rings can occur to form an NO₃−PAH adduct (step a), which can undergo back-decomposition to reactants (step b) in competition with bimolecular reactions with NO₂ (step c) and O₂ (step d). In addition, the adduct can undergo unimolecular reactions (step e).

In our experiments we saw both HNO₃ and NO₂ production. This is consistent with channels c and e. If these two channels are in fact dominant we would also expect to see nitro-pyrenes and hydroxyl-pyrenes as surface products. Future experiments focusing on the yields of these products would be beneficial.

Atmospheric Implications. *Comparison of the Different Oxidants.* Here we compare the importance of the different oxidants for heterogeneous oxidation of surface-bound PAHs in the atmosphere.

In Tables 2 and 3 we included the product of γ_0 and the average atmospheric concentrations of the gas-phase oxidants [oxidant]$_{atm}$. γ_0[oxidant]$_{atm}$ is a more relevant parameter for assessing the importance of the various radicals to atmospheric oxidation, compared with just γ_0, since the number of radicals lost to an organic surface will be proportional to γ_0[oxidant]$_{atm}$. The most important process will generally be the process with the largest γ_0[oxidant]$_{atm}$ and therefore the highest oxidative power. As can be seen from these calculations, the oxidative power of NO₃ is a factor of 60−1000 higher than that of all the other oxidants studied.

Lifetime (τ_{atm}) of Surface-Absorbed PAHs with Respect to the Different Oxidants. Above we used τ_{atm} to compare results

from different experiments when γ_0 was not measured. Here we use this value to assess the atmospheric importance of the various heterogeneous reactions. These lifetimes are reported in the last columns of Tables 2 and 3. On the basis of our data the atmospheric lifetime of PYR with respect to NO₃ heterogeneous loss is only seconds while all other lifetimes calculated from our data are greater than 12 min. In fact, in many cases the lifetimes of the other species based on our data are greater than hours. These results show that under typical atmospheric conditions at nighttime, NO₃ radicals (which are not present during the day) can be a more important sink for PAHs than NO₂, HNO₃, N₂O₅, or O₃ and may impact tropospheric lifetimes of surface-bound PAHs.

Direct Acting Mutagenicity of Wood Smoke and NO₃ Heterogeneous Chemistry. In a series of smoke chamber studies, Kamens et al.[51] have shown that the direct acting mutagenicity of wood smoke increased by 2−10-fold in the presence of O₃ and NO₂ (and also NO₃ and N₂O₅ since O₃ and NO₂ will lead to these oxidants). Our results suggest that the increased mutagenicity may have been in part due to the nitration by NO₃ radicals, since NO₃ can react more efficiently with PAHs in comparison with O₃, NO₂, and N₂O₅.

Summary and Conclusions

Reactive uptake coefficients were determined for the heterogeneous reactions of NO₃, N₂O₅, NO₂, HNO₃, and O₃ on three different solid PAH surfaces (pyrene, fluoranthene, and benz-[a]anthracene) at 273 K and at 293−297 K. This is the first measurement of the reactive uptake coefficient of N₂O₅ on PAH surfaces and only the second study to investigate the reactive uptake coefficient of NO₃ on surface-bound PAH material.[32] Reaction of NO₃ radicals with all three PAHs was observed to be very fast with the reactive uptake coefficient ranging from 0.059 (+0.11/−0.049) for benz[a]anthracene to 0.79 (+0.21/−0.67) for pyrene. In contrast to the NO₃ reactions, reactions of the different PAHs with the other gas-phase species (N₂O₅, NO₂, HNO₃, and O₃) were at or below the detection limit ($\gamma \leq 6.6 \times 10^{-5}$) in all cases, illustrating that these reactions are slow or do not occur. The uptake coefficients determined with NO₂, HNO₃, and O₃ showed no discrepancy with values obtained in previous studies. The reaction of NO₃ on all three PAH surfaces slowed down at 263 K after long NO₃ exposure times. While benz[a]anthracene showed a similar trend at room temperature, γ_{NO3} did not decrease on pyrene and fluoranthene after 60 min of NO₃ exposure at 296 K. This difference is thought to be due to the different volatility of the three different PAHs and their reaction products.

Our results show that under certain atmospheric conditions, NO₃ radicals may be a more important sink for PAHs than NO₂, HNO₃, N₂O₅, or O₃ and may impact tropospheric lifetimes of surface-bound PAHs. For example, calculations of oxidative power (γ_0[oxidant]$_{atm}$) and atmospheric lifetimes of PAHs with respect to the different gas-phase oxidants showed that under certain atmospheric conditions, NO₃ reactions should be a more important PAH loss process than the other oxidants studied. On the basis of our data, atmospheric lifetimes of surface-bound PAH material should be on the order of only seconds to minutes due to heterogeneous reactions with NO₃ radicals during the nighttime.

Furthermore, heterogeneous reactions between NO₃ and PAHs could also lead to sampling artifacts when measuring condensed phase PAHs in the atmosphere with filters. During the collection process, ambient air is drawn through the filters and the gas-phase oxidants can transform the collected particulate matter.

Polycyclic Aromatic Hydrocarbon Surfaces

J. Phys. Chem. A, Vol. 112, No. 14, 2008 **3113**

It has been shown that the reactions between O_3 and PAHs adsorbed on filters can lead to sampling artifacts (chemical loss and under-determination of PAHs).[43] The heterogeneous reaction between NO_3 and PAHs may also lead to sampling artifacts, since this reaction should be competitive with the O_3 and PAH heterogeneous reaction under certain conditions.

Most likely, there are no pure PAH surfaces in the atmosphere, but the presented results are important first outcomes in order to understand processes of heterogeneous PAH reactions under controlled laboratory conditions. More research on the heterogeneous reactions between NO_3 and PAHs on and in atmospherically realistic particles as well as analysis of condensed phase products is planned.

References and Notes

(1) Finlayson-Pitts, B. J.; Pitts, J. N. *Chemistry of the upper and lower atmosphere*; Academic Press: San Diego, 2000.

(2) Arey, J.; Atkinson, R.; Zielinska, B.; McElroy, P. A. *Environ. Sci. Technol.* **1989**, *23*, 321.

(3) Marr, L. C.; Dzepina, K.; Jimenez, J. L.; Reisen, F.; Bethel, H. L.; Arey, J.; Gaffney, J. S.; Marley, N. A.; Molina, L. T.; Molina, M. J. *Atmos. Chem. Phys.* **2006**, *6*, 1733.

(4) Reisen, F.; Arey, J. *Environ. Sci. Technol.* **2005**, *39*, 64.

(5) Ishii, S.; Hisamatsu, Y.; Inazu, K.; Kadoi, M.; Aika, K. I. *Environ. Sci. Technol.* **2000**, *34*, 1893.

(6) Lewis, A. C.; Bartle, K. D.; Pilling, M. J. *Polycyclic Aromat. Compd.* **2002**, *22*, 175.

(7) Yang, H. H.; Tsai, C. H.; Chao, M. R.; Su, Y. L.; Chien, S. M. *Atmos. Environ.* **2006**, *40*, 1266.

(8) Ammann, M.; Pöschl, U.; Rudich, Y. *Phys. Chem. Chem. Phys.* **2003**, *5*, 351.

(9) Lam, B.; Diamond, M. L.; Simpson, A. J.; Makar, P. A.; Truong, J.; Hernandez-Martinez, N. A. *Atmos. Environ.* **2005**, *39*, 6578.

(10) Simpson, A. J.; Lam, B.; Diamond, M. L.; Donaldson, D. J.; Lefebvre, B. A.; Moser, A. Q.; Williams, A. J.; Larin, N. I.; Kvasha, M. P. *Chemosphere* **2006**, *63*, 142.

(11) Bamford, H. A.; Baker, J. E. *Atmos. Environ.* **2003**, *37*, 2077.

(12) Moise, T.; Rudich, Y. *Geophys. Res. Lett.* **2001**, *28*, 4083.

(13) Dubowski, Y.; Vieceli, J.; Tobias, D. J.; Gomez, A.; Lin, A.; Nizkorodov, S. A.; McIntire, T. M.; Finlayson-Pitts, B. J. *J. Phys. Chem. A* **2004**, *108*, 10473.

(14) Kahan, T. F.; Kwamena, N. O. A.; Donaldson, D. J. *Atmos. Environ.* **2006**, *40*, 3448.

(15) Mmereki, B. T.; Donaldson, D. J.; Gilman, J. B.; Eliason, T. L.; Vaida, V. *Atmos. Environ.* **2004**, *38*, 6091.

(16) Esteve, W.; Budzinski, H.; Villenave, E. *Atmos. Environ.* **2006**, *40*, 201.

(17) Esteve, W.; Budzinski, H.; Villenave, E. *Atmos. Environ.* **2004**, *38*, 6063.

(18) Bertram, A. K.; Ivanov, A. V.; Hunter, M.; Molina, L. T.; Molina, M. J. *J. Phys. Chem. A* **2001**, *105*, 9415.

(19) Arens, F.; Gutzwiller, L.; Gaggeler, H. W.; Ammann, M. *Phys. Chem. Chem. Phys.* **2002**, *4*, 3684.

(20) Ishii, S.; Hisamatsu, Y.; Inazu, K.; Kobayashi, T.; Aika, K. *Chemosphere* **2000**, *41*, 1809.

(21) Inazu, K.; Kobayashi, T.; Hisamatsu, Y. *Chemosphere* **1997**, *35*, 607.

(22) Inazu, K.; Tsutsumi, N.; Aika, K. I.; Hisamatsu, Y. *Polycyclic Aromat. Compd.* **2000**, *20*, 191.

(23) Pöschl, U.; Letzel, T.; Schauer, C.; Niessner, R. *J. Phys. Chem. A* **2001**, *105*, 4029.

(24) Kwamena, N. O. A.; Thornton, J. A.; Abbatt, J. P. D. *J. Phys. Chem. A* **2004**, *108*, 11626.

(25) Mmereki, B. T.; Donaldson, D. J. *J. Phys. Chem. A* **2003**, *107*, 11038.

(26) Alebic-Juretic, A.; Cvitas, T.; Klasinc, L. *Environ. Sci. Technol.* **1990**, *24*, 62.

(27) Pitts, J. N.; Paur, H. R.; Zielinska, B.; Arey, J.; Winer, A. M.; Ramdahl, T.; Mejia, V. *Chemosphere* **1986**, *15*, 675.

(28) Van Vaeck, L.; Van Cauwenberghe, K. *Atmos. Environ.* **1984**, *18*, 323.

(29) Vione, D.; Barra, S.; De Gennaro, G.; De Rienzo, M.; Gilardoni, S.; Perrone, M. G.; Pozzoli, L. *Ann. Chim.* **2004**, *94*, 257.

(30) Pitts, J. N.; Zielinska, B.; Sweetman, J. A.; Atkinson, R.; Winer, A. M. *Atmos. Environ.* **1985**, *19*, 911.

(31) Kamens, R. M.; Guo, J.; Guo, Z.; Mcdow, S. R. *Atmos. Environ., Part a: Gen. Top.* **1990**, *24*, 1161.

(32) Mak, J.; Gross, S.; Bertram, A. K. *Geophys. Res. Lett.* **2007**, *34*, L10804.

(33) Knopf, D. A.; Anthony, L. M.; Bertram, A. K. *J. Phys. Chem. A* **2005**, *109*, 5579.

(34) Knopf, D. A.; Mak, J.; Gross, S.; Bertram, A. K. *Geophys. Res. Lett.* **2006**, *33*, L17816.

(35) Huey, L. G.; Hanson, D. R.; Howard, C. J. *J. Phys. Chem.* **1995**, *99*, 5001.

(36) Brown, R. L. *J. Res. Natl. Bur. Standards* **1978**, *83*, 1.

(37) Aubin, D. G.; Abbatt, J. P. *J. Phys. Chem. A* **2003**, *107*, 11030.

(38) Schott, G.; Davidson, N. *J. Am. Chem. Soc.* **1958**, *80*, 1841.

(39) Rudich, Y.; Talukdar, R. K.; Imamura, T.; Fox, R. W.; Ravishankara, A. R. *Chem. Phys. Lett.* **1996**, *261*, 467.

(40) Atkinson, R. *J. Phys. Chem. Ref. Data* **1991**, *20*, 459.

(41) Paz, Y.; Trakhtenberg, S.; Naaman, R. *J. Phys. Chem.* **1992**, *96*, 10964.

(42) Paz, Y.; Trakhtenberg, S.; Naaman, R. *J. Phys. Chem.* **1994**, *98*, 13517.

(43) Schauer, C.; Niessner, R.; Pöschl, U. *Environ. Sci. Technol.* **2003**, *37*, 2861.

(44) Longfellow, C. A.; Ravishankara, A. R.; Hanson, D. R. *J. Geophys. Res.-Atmos.* **2000**, *105*, 24345.

(45) Nielsen, T. *Environ. Sci. Technol.* **1984**, *18*, 157.

(46) Vione, D.; Maurino, V.; Minero, C.; Pelizzetti, E. *Environ. Sci. Technol.* **2005**, *39*, 1101.

(47) Sasaki, J.; Aschmann, S. M.; Kwok, E. S. C.; Atkinson, R.; Arey, J. *Environ. Sci. Technol.* **1997**, *31*, 3173.

(48) Calvert, J. G.; Atkinson, R.; Becker, K. H.; Kamens, R. M.; Seinfeld, J. H.; Wallington, T. J.; Yarwood, G. *The mechanisms of atmospheric oxidation of aromatic hydrocarbons*; Oxford University Press: New York, 2002.

(49) Atkinson, R.; Arey, J. *Environ. Health Perspect.* **1994**, *102*, 117.

(50) Kwok, E. S. C.; Harger, W. P.; Arey, J.; Atkinson, R. *Environ. Sci. Technol.* **1994**, *28*, 521.

(51) Kamens, R. M.; Rives, G. D.; Perry, J. M.; Bell, D. A.; Paylor, R. F.; Goodman, R. G.; Claxton, L. D. *Environ. Sci. Technol.* **1984**, *18*, 523.